ChemPubSoc Europe

DOI: 10.1002/open.201700165

Open Access ChemistryOPEN Full Papers

# Magnetic Nature of the $Cr^{III}$–$Ln^{III}$ Interactions in $[Cr^{III}_2Ln^{III}_3]$ Clusters with Slow Magnetic Relaxation

Xiao-Qing Zhao,*[a, b] Shuo Xiang,[a] Jin Wang,[a] Dong-Xu Bao,[a] and Yun-Chun Li[a]

Two 3*d*-4*f* hetero-metal pentanuclear complexes with the formula {$[Cr^{III}_2Ln^{III}_3L_{10}(OH)_6(H_2O)_2]Et_3NH$} [Ln = Tb (**1**), Dy (**2**); HL = pivalic acid, $Et_3N$ = triethylamine] have been produced. The metal core of each cluster is made up of a trigonal bipyramid with three $Ln^{III}$ ions (plane) and two $Cr^{III}$ ions (above and below) held together by six $\mu_3$-OH bridges. Also reported with this series is the diamagnetic $Cr^{III}$–$Y^{III}$ analogue (**3**). Fortunately, we successfully prepared $Al^{III}$–$Ln^{III}$ analogues with the formula {$[Al^{III}_2Ln^{III}_3L_{10}(OH)_6(H_2O)_2]Et_3NH{\cdot}H_2O$} [Ln = Tb (**4**), Dy (**5**)], containing diamagnetic $Al^{III}$ ions, which can be used to evaluate the $Cr^{III}$–$Ln^{III}$ magnetic nature through a diamagnetic substitution method. Subsequently, static (dc) magnetic susceptibility studies reveal dominant ferromagnetic interactions between $Cr^{III}$ and $Ln^{III}$ ions. Dynamic (ac) magnetic susceptibility studies show frequency-dependent out-of-phase ($\chi''$) signals for $[Cr^{III}_2Tb^{III}_3]$ (**1**), $[Cr^{III}_2Dy^{III}_3]$ (**2**), and $[Al^{III}_2Dy^{III}_3]$ (**5**), which are derived from the single-ion behavior of $Ln^{III}$ ions and/or the $Cr^{III}$–$Ln^{III}$ ferromagnetic interactions.

## 1. Introduction

Molecule-based magnetic materials have become an important area in modern coordination chemistry over the past two decades; therein, single-molecule magnets (SMMs) exhibiting slow magnetic relaxation have attracted great concern, because of future prospects in information storage techniques.[1–4] Indeed, SMMs are a molecular approach to nanoscale particles, which can be magnetized in an external magnetic field and they retain magnetization when the field is turned off. Such behavior is derived from the combination of the large ground-state spin (*S*) and a large magnetic anisotropy of the Ising (easy-axis) type with a negative zero-field splitting parameter, *D*. This leads to an energy barrier ($U_{eff}$) to magnetic relaxation with exchange interactions between the magnetic centers.[5]

Since the first discovery of $Mn_{12}$ SMM,[6–8] coordination clusters containing $Mn^{III}$ ions are the richest family of SMMs, owing to its favorable Ising anisotropy;[9–16] however, SMMs with other 3*d* ions have been successfully isolated, such as $Fe^{III}$,[17–20] $Co^{II}$,[21–25] and $Ni^{II}$,[26–31] all of which possess anisotropic characteristics. In 2003, a $Tb^{III}$ complex displayed SMM behavior,[32] opening the upsurge in searching for lanthanide-based SMMs; since then, plenty of lanthanide-based SMMs have been reported, proving that lanthanide ions are good candidates to construct SMMs, owing to their large magnetic moments and anisotropy.[33–41]

Among the many lanthanide-based complexes, 3*d*–4*f* coordination clusters have been considered one of the most interesting molecular systems for magnetic studies.[42–60] The strategy for constructing 3*d*–4*f* coordination clusters is to build metal cores with organic ligands, which act not only as bridging ligands to bridge 3*d* and 4*f* ions, but also as peripheral ligands to separate the discrete species from each other. However, such systems are quite difficult to analyze because: i) it is well-known that lanthanide ions have contracted *f*-orbitals and the magnetic exchange interactions between them are extremely weak, which has been reported for the majority of lanthanide-based clusters; ii) the 3*d*–4*f* exchange interactions are always weak and difficult to determine, because of the complicated magnetic interactions in this system (*d*–*d*, *d*–*f*, and *f*–*f* interactions) and the intrinsic nature of 4*f* ions with an orbital contribution to their ground states.[61]

To analyze the 3*d*–4*f* exchange interactions, diamagnetic substitution is a successful approach to address the problem, which consists of comparing the magnetic behaviors of two isostructural systems (one with a 4*f* ion and a second paramagnetic center; the other with a 4*f* ion and a diamagnetic center) to garner insight into the magnetic nature between 3*d* and 4*f* ions. The comparison of two systems will eliminate the contribution of the spin–orbit coupling of 4*f* ions, thus revealing the magnetic nature of the 3*d*–4*f* interactions. However, to date, the use of this approach to obtain the magnetic nature of 3*d*–4*f* interactions is rather rare, owing to the complexity in obtaining the diamagnetic analogues, and then only a few 3*d*–

[a] Dr. X.-Q. Zhao, S. Xiang, J. Wang, D.-X. Bao, Y.-C. Li
College of Science, Sichuan Agricultural University
Ya'an 625014 (P.R. China)
E-mail: zhaoxiaoqing@sicau.edu.cn

[b] Dr. X.-Q. Zhao
Key Laboratory of Advanced Energy Materials Chemistry
Ministry of Education, Nankai University
Tianjin 300071 (P.R. China)

Supporting Information and the ORCID identification number(s) for the author(s) of this article can be found under https://doi.org/10.1002/open.201700165.

4*f* coordination systems have been successfully applied to diamagnetic substitution to determine the nature of magnetic exchange interaction between 3*d* and 4*f* ions.[62–67] For instance, we use the diamagnetic substitution to obtain the magnetic nature between 3*d* and 4*f* ions of the hetero-metal $Mn^{II}$–$Ln^{III}$ family.[67]

On the other hand, much work has concentrated on mixing 4*f* ions with anisotropic 3*d* ions to prepare the former 3*d*-based SMMs; however, some isotropic ions can also be favorable in 3*d*–4*f* coordination clusters with enhanced SMM properties.[68–75] Since the $[Cr^{III}_4Dy^{III}_4]$ SMM was reported,[68] 3*d*–4*f* SMMs containing $Cr^{III}$ ions have drawn great attention.[69–75] More recently, a rare $[Cr^{III}_2Dy^{III}_2]$ SMM with a high $U_{eff}$ of 77 K and large coercive magnetic fields was synthesized, which can significantly reduce the quantum tunneling of magnetization (QTM) due to the exchange interaction between $Cr^{III}$ and $Dy^{III}$ ions.[74] Following work showed that the $U_{eff}$ was related to the magnitude of exchange between magnetic centers by comparing it to two families of $Cr^{III}$-containing SMMs.[75] Interestingly, incorporating a diamagnetic metal ion provides a potential avenue to improve the $U_{eff}$ parameter in lanthanide-based SMMs.[76–78]

Inspired by these aforementioned aspects, we chose the isotropic $Cr^{III}$ ion as a 3*d* metal ion to fabricate 3*d*–4*f* clusters, aiming to obtain novel SMMs. As a result, we obtained two hetero-metal $Cr^{III}$–$Ln^{III}$ clusters with a $[Cr^{III}_2O_6Ln^{III}_3]$ core [Ln = Tb (**1**) and Dy (**2**)], showing SMM-like behavior. To understand the magnetic interactions between $Cr^{III}$ and $Ln^{III}$ ions, the diamagnetic $Y^{III}$ and $Al^{III}$ ions were expected to substitute $Ln^{III}$ and $Cr^{III}$ ions, respectively, to obtain analogues. Fortunately, the corresponding $Cr^{III}$–$Y^{III}$ (**3**) and $Al^{III}$–$Ln^{III}$ (**4** and **5**) analogues were successfully isolated and characterized. Static (dc) magnetic studies suggest strong ferromagnetic interactions between $Cr^{III}$ and $Ln^{III}$ ions within **1** and **2**. Dynamic (ac) magnetic properties show that complexes **1**, **2**, and **5** display slow magnetic relaxation.

## 2. Results and Discussion

### 2.1. Syntheses

Hetero-metal pentanuclear 3*d*–4*f* complexes with the general formula $[Cr^{III}_2Ln^{III}_3L_{10}(OH)_6(H_2O)_2]Et_3NH$ [where Ln = Tb (**1**), Dy (**2**)] have been produced by using a solution-based method. The reaction of $CrCl_3{\cdot}6H_2O$, $Ln(NO_3)_3{\cdot}6H_2O$, and HL in a 5:3:10 molar ratio with $Et_3N$ in mixed $CH_3CN$ and $CH_2Cl_2$ (1:1) gave a light purple solution, from which well-shaped purple crystals were obtained after several days. Fortunately, using $Y(NO_3)_3{\cdot}6H_2O$ instead of $Ln(NO_3)_3{\cdot}6H_2O$ produced the $Cr^{III}$–$Y^{III}$ complex (**3**); furthermore, when replacing $CrCl_3{\cdot}6H_2O$ with $AlCl_3$ as the original material, the corresponding $Al^{III}$–$Ln^{III}$ analogues with the formula $\{[Al^{III}_2Ln^{III}_3L_{10}(OH)_6(H_2O)_2]Et_3NH{\cdot}H_2O\}$ [Ln = Tb (**4**), Dy (**5**)] were obtained successfully.

### 2.2. Crystal Structures of Complexes 1–5

These hetero-metal complexes are isostructural and crystallize in tetragonal space group $P4_2/nmc$. The structure of complex **1** is described here as a representative, in which the $Cr^{III}$ and $Tb^{III}$ ions are held together by six $\mu_3$-OH bridges (O1, O2, and symmetry related) to display a trigonal dipyramidal configuration (Figure 1). The Tb1, Tb2, and Tb1A centers locate at the equatorial plane to form a nearly perfect trianglular plane with

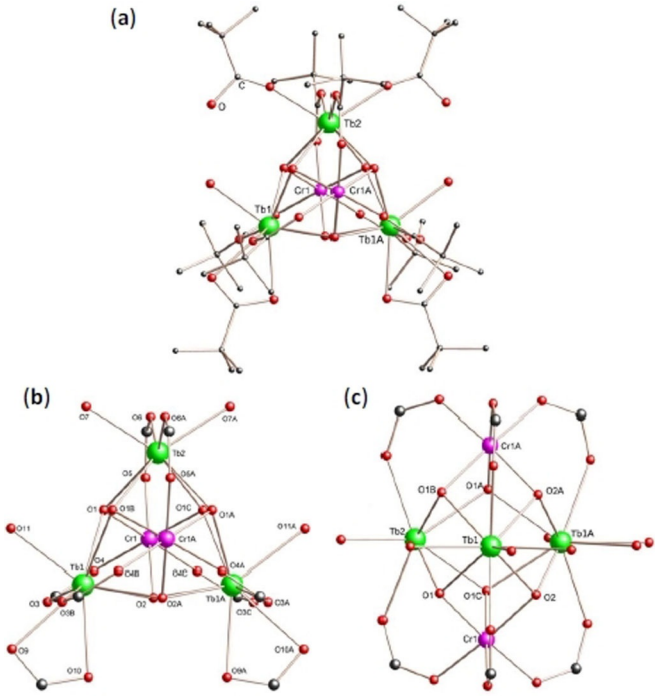


**Figure 1.** a) Molecular structure of **1**, representing the common topology observed in complexes **1**–**3**; H atoms and solvent molecules are omitted for clarity. b) Top view of the core with the atom labels. c) Side view of the core, showing the trigonal bipyramidal configuration.

lengths of 3.960–3.974 Å and angles of approximately 60°, whereas Cr1 and Cr1A occupy the axial sites, and six $\mu_3$-OH bridge two $Tb^{III}$ ions to each $Cr^{III}$ ion, forming a $[Cr^{III}_2O_6Tb^{III}_3]$ core with a trigonal dipyramidal shape (Figure S1). The Tb···Cr distances are 3.478 (Cr1···Tb1) and 3.461 Å (Cr1···Tb2), and that of Cr···Cr is 5.217 Å. The Cr···Tb···Cr angles are 97.16° (Cr1···Tb1···Cr1A) and 97.86° (Cr1···Tb2···Cr1A), whereas the Cr···O···Tb and Tb···O···Tb angles are in the ranges of 103.13–104.15° and 109.32–110.11°, respectively (other Cr–Ln complexes are detailed in Tables S1 and S2). This core is further ligated by ten $L^-$ ligands and two terminal water molecules around the periphery. Among the ten $L^-$ ligands, six $L^-$ ligands adopt a *syn–syn* mode to bridge neighboring $Cr^{III}$ and $Tb^{III}$ ions, and two bidentately chelate one $Tb^{III}$ center, whereas the left two act as monodentate ligands to coordinate with one $Tb^{III}$ center.

The asymmetric unit consists of a quarter of the molecule, and there is one crystallographically independent $Cr^{III}$ and two $Tb^{III}$ ions in the molecular structure. The $Cr^{III}$ center has close to the perfect octahedral geometry involving $O_6$ donor sets, whereas the larger $Tb^{III}$ ions take up the nine and eight coordination sets, respectively, for Tb1 and Tb2, involving all O donor combinations. $Tb^{III}$ ions were systemically analyzed by using

SHAPE 2.1 software,[79] resulting in a capped square antiprism ($D_{4v}$, with a value of 1.320) and a square antiprism ($D_{4d}$, with a value of 0.943) for Tb1 and Tb2, respectively, as shown in Figure 2. The octahedral geometry around Cr1 is completed by

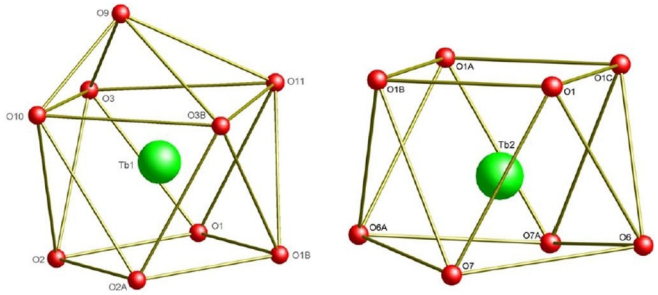


**Figure 2.** The coordination spheres around Tb1 and Tb2 in **1**.

six O atoms from three $\mu_3$-OH (O1, O2, O1C) and three carboxylate O atoms (O4, O5, O4C) of three $L^-$ ligands. The bond distances range from 1.977(6) to 1.983(5) Å, whereas the *trans* angles are close to linearity [175.77(27) and 176.256(181)°]. The nine coordination sets around the Tb1 ion contain four $\mu_3$-OH (O1, O2, O1B, O2A), two carboxylate O atoms (O3, O3B) of two carboxylate groups in *syn–syn* mode, one bidentate carboxylate group (O9, O10), and a terminal water molecule (O11). For Tb2, the difference from the Tb1 ion is that two monodentate carboxylate groups (O7, O7A) replace the bidentate carboxylate group and the coordinated water molecule is removed.

The $Al^{III}_2Ln^{III}_3$ analogues (**4** and **5**) with the replacement of $Cr^{III}$ by $Al^{III}$ display the similar structures (Figure S2). The $Al^{III}$ centers are six-coordinate with octahedral geometry, while the $Ln^{III}$ centers have two coordination environments: nine donor sets with capped square antiprism (Ln1) and eight ones for square-antiprism (Ln2), as $Cr^{III}_2Ln^{III}_3$ series. Their relevant metrical parameters are shown in Table S1 and S2. The packing structure of complexes (**1**–**5**) shows 1D channels along *c* axis, and suggests that the counter ion ($Et_3NH$) and lattice water molecules locate in the channels (Figure S3).

### 2.3. Thermogravimmetric and Powder X-ray Diffraction Analyses

The thermogravimetric (TG) analyses of complexes **1**–**5** were measured under a $N_2$ atmosphere with a heating rate of 10 °C min$^{-1}$ (Figure S4). The weight losses for complexes **1**–**5** were equal to 5.7% (170 °C), 5.5% (170 °C), 5.5% (170 °C), 6.3% (150 °C), and 7.6% (150 °C), which can be assigned to the loss of $Et_3N$ for complexes **1**–**3** and $Et_3N$ and $H_2O$ for complexes **4** and **5** (calcd 5.5, 5.5, 6.2, 6.6, 6.6%). Further weight loss gives rise to the decomposition of complexes **1**–**5**.

Powder X-ray diffraction (PXRD) measurements of complexes **1**–**5** in crystalline samples were carried out and the results are shown in Figures S5 and S6. The experimental PXRD patterns are consistent with the simulated pattern (complexes **1** and **4**, respectively). Minor inconsistencies between experimental and simulation data have been observed in the intensity and shape of peaks, which are attributed to the different orientation of crystals in crystalline samples. All crystallographic data are detailed in Table 1.

### 2.4. Magnetic Properties

It is well-known that lanthanide-based complexes exhibit unique magnetic properties for their rather large and aniso-

**Table 1.** Crystallographic data for complexes **1**–**5**.

| | **1** | **2** | **3** | **4** | **5** |
|---|---|---|---|---|---|
| Formula | $Cr_2Tb_3$ $C_{56}H_{116}O_{28}N$ | $Cr_2Dy_3$ $C_{56}H_{116}O_{28}N$ | $Cr_2Y_3$ $C_{56}H_{116}O_{28}N$ | $Al_2Tb_3$ $C_{56}H_{118}O_{29}N$ | $Al_2Dy_3$ $C_{56}H_{118}O_{29}N$ |
| $M_r$ [g mol$^{-1}$] | 1832.25 | 1842.99 | 1622.22 | 1800.23 | 1810.97 |
| $T$ [K] | 153(2) | 127.90(14) | 143.05(10) | 128.15(10) | 134(2) |
| Crystal system | tetragonal | | | | |
| Space group | $P4_2/nmc$ | | | | |
| $a$ [Å] | 18.5502(4) | 18.2504(3) | 18.4885(6) | 18.5518(3) | 18.5559(4) |
| $b$ [Å] | 18.5502(4) | 18.2504(3) | 18.4885(6) | 18.5518(3) | 18.5559(4) |
| $c$ [Å] | 29.6308(6) | 29.7619(8) | 29.6790(10) | 29.2890(6) | 29.3126(5) |
| $\alpha=\beta=\gamma$ [°] | 90.00 | | | | |
| $V$ [Å$^3$] | 10196.3(5) | 9913.0(4) | 10145.0(7) | 10080.3(4) | 10093.0(4) |
| $Z$ | 4 | | | | |
| $\rho_{calcd}$ [g cm$^{-3}$] | 1.194 | 1.235 | 1.062 | 1.186 | 1.192 |
| $\mu$ [mm$^{-1}$] | 2.315 | 2.502 | 1.960 | 2.156 | 2.272 |
| $F$(000) | 3704.0 | 3716.0 | 3392.0 | 3656.0 | 3668.0 |
| $2\theta_{max}$ [°] | 50.02 | 50.02 | 50.02 | 50.02 | 50.01 |
| Refl. collected/unique | 32433/4782 | 19953/4672 | 23049/4720 | 20156/4691 | 20680/4695 |
| $R$(int) | 0.0500 | 0.0620 | 0.0835 | 0.0455 | 0.0529 |
| GOF on $F^2$ | 1.074 | 1.063 | 1.058 | 1.047 | 1.043 |
| $R_1/wR_2$ [$I>2\sigma(I)$] | 0.0586/0.1438 | 0.0940/0.2299 | 0.0819/0.2356 | 0.0528/0.1270 | 0.0454/0.1085 |
| $R_1/wR_2$ (all data) | 0.0709/0.1555 | 0.1397/0.2729 | 0.1266/0.2678 | 0.0674/0.1377 | 0.0611/0.1185 |
| Largest difference peak/hole [eÅ$^{-3}$] | 2.54/−1.07 | 2.12/−1.33 | 1.31/−0.62 | 1.15/−-1.12 | 1.16/−0.71 |

tropic magnetic moments. Over the past two decades, a large number of lanthanide-based complexes in which the $Ln^{III}$ ion is exchange-coupled with a second spin carrier, such as transition-metal ion (M) and organic radical, have been obtained; however, except for isotropic $Gd^{III}$, little is known about the nature and magnitude of the magnetic interactions within these complexes. This is because the thermal population of the $M_J$ levels of the $Ln^{III}$ ions complicate the magnetic properties, making the analysis of the magnetic behaviors of M···$Ln^{III}$ coupling much more difficult. Herein, we successfully applied diamagnetic substitution to get insight into the magnetic nature of $Cr^{III}$–$Ln^{III}$ interactions through the comparison of the magnetic behaviors of $[Cr^{III}_2Ln^{III}_3]$ and $[Al^{III}_2Ln^{III}_3]$ complexes.

### 2.5. Static (dc) Magnetic Susceptibility Data

The temperature-dependent magnetic susceptibilities of complexes **1**–**5** were collected in the field of 1000 Oe. Plots of $\chi_m T$ or $\Delta\chi_m T$ versus $T$ are shown in Figures 3–6, and the magnetic data of complexes **1**–**5** are summarized in Table 2.

As shown in Figure 3, complexes **1** and **2** have room-temperature $\chi_m T$ values of 35.98 and 41.75 $cm^3 mol^{-1} K$, respectively, which are smaller than the expected values for two uncoupled $Cr^{III}$ ions and three respective $Ln^{III}$ ions (Table 2), maybe because of the spin-orbit coupling of lanthanide ions. The curves of complexes **1** and **2** display similar features. As the temperature is decreased, the $\chi_m T$ values are roughly constant from 300 to 50 K and then increase more and more rapidly, reaching a maximum value at 1.8 K. In fact, there is a slight gradual decrease between room temperature and 100 K, which may be attributed to the thermal depopulation of the Stark sublevels of the anisotropic $Ln^{III}$ ions. The continual increase of the $\chi_m T$ values for **1** and **2** indicate that non-negligible and significant magnetic exchange interactions are present between the $Dy^{III}$/$Tb^{III}$ and the $Cr^{III}$ ions. Within the trigonal bipyramidal structure, the interaction between two $Cr^{III}$ ions, separated by more than 5 Å, is certainly very small (as following depicted) compared to the $Cr^{III}$···$Ln^{III}$ and $Ln^{III}$···$Ln^{III}$ interactions through the $\mu_3$-O bridges. Therefore, the $Cr^{III}$···$Ln^{III}$ and/or $Ln^{III}$···$Ln^{III}$ interactions within complexes **1** and **2** are ferromagnetic.

Complex **3** incorporates the diamagnetic $Y^{III}$ and paramagnetic $Cr^{III}$ ions into one system, and can give some insight into the nature of the $Cr^{III}$···$Cr^{III}$ magnetic interaction. As shown in Figure 4, the room temperature $\chi_m T$ value is 3.45 $cm^3 mol^{-1} K$, which is consistent with the theoretical value of 3.75 $cm^3 mol^{-1} K$ of two uncoupled $Cr^{III}$ ions. As the temperature is decreased, the $\chi_m T$ value remains constant until 50 K, and then decreases to reach 2.10 $cm^3 mol^{-1} K$ at the lowest temperature. The decrease at the lowest temperature might be caused by the antiferromagnetic coupling or zero-field splitting on $Cr^{III}$ centers. $Cr^{III}_2Y^{III}_3$ can be viewed as a dimer of $Cr^{III}$ with a pair of exchange-coupled spin-only $S = 3/2$ spins. The

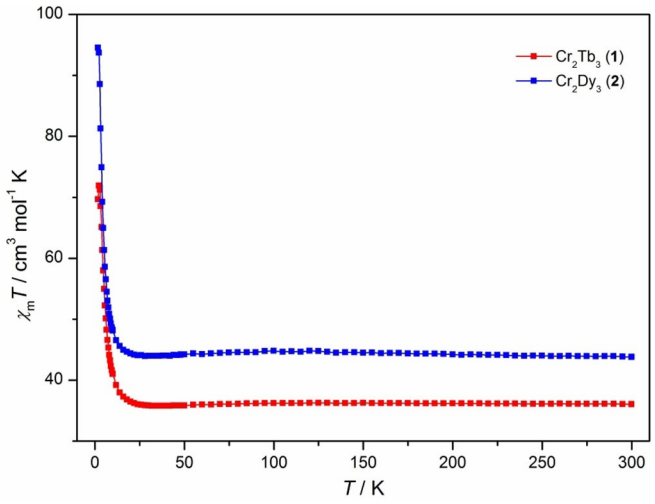


**Figure 3.** Plots of $\chi_m T$ versus $T$ for complexes **1** and **2** at 1000 Oe.

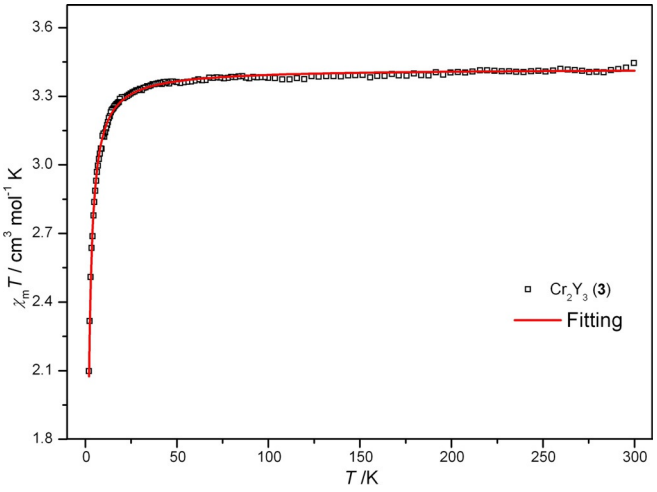


**Figure 4.** Temperature dependence of $\chi_m T$ under a 0.1 T applied field for **3**, and the red line shows the fitting.

**Table 2.** Key magnetic data for complexes **1**–**5**.

| Complex $[M^{III}_2Ln^{III}_3]$ | Ground multiplet of $Ln^{III}$ | $g_J$ | Curie Constant for $Ln^{III}$ ion[a] [$cm^3 mol^{-1} K$] | Predicted $\chi_m T$[a] [$cm^3 mol^{-1} K$] | Measured $\chi_m T$[a] [$cm^3 mol^{-1} K$] | Measured $\chi_m T$[b] [$cm^3 mol^{-1} K$] |
|---|---|---|---|---|---|---|
| **1** $[Cr^{III}_2Tb^{III}_3]$ | $^7S_6$ | 3/2 | 11.82 | 39.21 | 35.98 | 69.66 |
| **2** $[Cr^{III}_2Dy^{III}_3]$ | $^6H_{15/2}$ | 4/3 | 14.17 | 46.26 | 41.75 | 94.51 |
| **3** $[Cr^{III}_2Y^{III}_3]$ | - | $g_{Cr} = 2$ | 0 | 3.75 | 3.45 | 2.10 |
| **4** $[Al^{III}_2Tb^{III}_3]$ | $^7S_6$ | 3/2 | 11.82 | 35.46 | 32.63 | 18.68 |
| **5** $[Al^{III}_2Dy^{III}_3]$ | $^6H_{15/2}$ | 4/3 | 14.17 | 42.51 | 37.89 | 24.23 |

[a] At 300 K. [b] At 1.8 or 2.0 K.

susceptibility is given in the exchange spin Hamiltonian written as $H_{ex} = -2J\ S_1 \cdot S_2$ and can be fitted to give $J = -0.22(6)\ cm^{-1}$ and $g = 1.90(9)$ (Figure 4), showing the weak antiferromagnetic Cr–Cr interactions. Furthermore, the fitting of the Curie–Weiss law gives $\theta = -0.96$ K and $C = 3.11\ cm^3\ mol^{-1}\ K$ (Figure S7), and the negative $\theta$ confirms the antiferromagnetic interaction.

The plots of $\chi_m T$ versus $T$ of the corresponding $Al^{III}$–$Ln^{III}$ series (complexes **4** and **5**) are displayed in Figure 5, and the

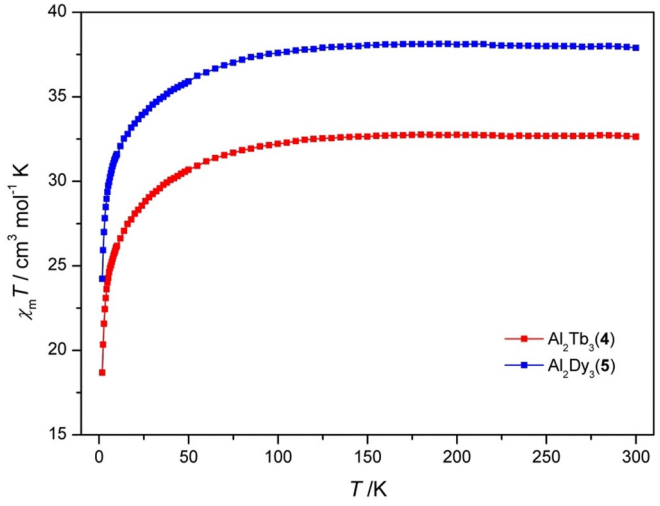


**Figure 5.** Plots of $\chi_m T$ versus $T$ for complexes **4** and **5** at 1000 Oe.

$\chi_m T$ values of 32.63 and 37.89 $cm^3\ mol^{-1}\ K$ at 300 K are smaller than the predicted values of three uncoupled $Ln^{III}$ ions (Table 2), maybe owing to the strong spin-orbit coupling of lanthanide ions. The $\chi_m T$ values of complexes **4** and **5** decrease slightly as the temperature decreases to 100 K, and then drop rapidly to reach minimum values at the lowest temperature (Table 2). For the $Al^{III}$–$Ln^{III}$ series, the $Al^{III}$ ion is diamagnetic, thus the $Ln^{III}$···$Ln^{III}$ interactions may play an important role in the magnetic behavior. Considering the magnetic results and the thermal depopulation of the $Ln^{III}$ ions, the $Ln^{III}$···$Ln^{III}$ interactions within complexes **4** and **5** cannot be determined.

In the vast majority of $Cr^{III}Ln^{III}$ systems, the $\chi_m T$ values decreased upon lowering the temperature, which suggests the spin-orbit coupling of the $Ln^{III}$ ions and/or antiferromagnetic interactions between metal ions are dominant within these systems. In some $Cr^{III}Ln^{III}$ cases, the $\chi_m T$ products presented a small rise before a continual decrease, indicting the presence of weak ferromagnetic interactions, but no examples use diamagnetic substitution to evaluate the magnetic coupling between $Cr^{III}$ and $Ln^{III}$ ions.[68–72,80–82] Compared to these complexes, it is the first time diamagnetic substitution is used to determine the strong ferromagnetic interactions between $Cr^{III}$ and $Ln^{III}$ ions within complexes **1** and **2**.

To obtain new insight into the nature of the M–$Ln^{III}$ (M = a transition-metal ion or an organic radical) interactions, the method of diamagnetic ion substitution addressed by Kahn et al. proved to be effective.[62] Here, the nature of the magnetic interactions between $Cr^{III}$ and $Ln^{III}$ within complexes **1** and **2** was investigated by comparing the magnetic susceptibilities of $Cr^{III}_2Ln^{III}_3$ with those of corresponding $Al^{III}_2Ln^{III}_3$ and $Cr^{III}_2Y^{III}_3$ analogues involving the diamagnetic $Al^{III}$ and $Y^{III}$ ions, respectively. $\Delta\chi_m T$ is defined as $\Delta\chi_m T = (\chi_m T)_{Cr_2Ln_3} - (\chi_m T)_{Al_2Ln_3} - (\chi_m T)_{Cr_2Y_3}$ and was obtained experimentally, which may eliminate the crystal-field contribution of $Ln^{III}$ ions, and then the profile for $\Delta\chi_m T$ could be characteristic of the $Cr^{III}$···$Ln^{III}$ interactions within the complexes. The plots of $\Delta\chi_m T$ versus $T$ are displayed in Figure 6. The $\Delta\chi_m T$ values for complexes with Tb and Dy increase slightly from 300 to about 100 K, and increase more and more rapidly as the temperature approaches zero. The profile of those curves clearly indicates strong ferromagnetic interactions between the $Cr^{III}$ and $Ln^{III}$ ions within the corresponding complexes.

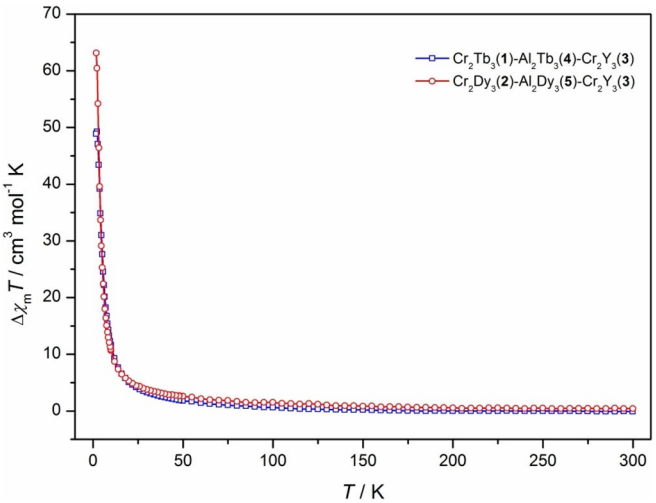


**Figure 6.** Plots of $\Delta\chi_m T$ defined as $\Delta\chi_m T = (\chi_m T)_{Cr_2Ln_3} - (\chi_m T)_{Al_2Ln_3} - (\chi_m T)_{Cr_2Y_3}$ versus $T$.

The field dependence of magnetization was performed for complexes **1**–**5**, and the corresponding field-independent isothermal magnetization data are shown in Figures S8 and S9. The $M$ versus $H$ plots of complexes **1**, **2**, **4**, and **5** show sharp increases with increasing $H$ at low fields and low temperature, and then linear increases with larger fields. The magnetizations of complexes **1**, **2**, **4**, and **5** are not saturated even at 2 K under 7 T (Figure S8), indicating the presence of magnetic anisotropy, as expected for $Ln^{III}$-based complexes. The plots of $M$ versus $H/T$ show non-superposed curves (Figure S9), further confirming the highly anisotropic ground state and/or low-lying excited states. The plot of $M$ versus $H$ at 2 K for complex **3** is shown in Figure S10, and the magnetization significant is not saturated under 7 T, reaching a value of 5.44 $N\beta$ at 7 T.

### 2.6. Dynamic (ac) Magnetic Susceptibility Data

To probe the presence of slow magnetic relaxations in these systems, and thus the presence of SMM behaviors, ac magnetic susceptibilities were performed on these complexes at zero dc field. In the $Cr^{III}$–$Ln^{III}$ series, complexes **1** and **2** exhibit frequency-dependent out-of-phase ($\chi''$) signals (Figures 7 and 8),

whereas complex **3** has no frequency-dependent signals under the experimental conditions (Figure S11). Meanwhile, among the $Al^{III}$–$Ln^{III}$ series, complex **5** with $Dy^{III}$ exhibits frequency-dependent $\chi'$ and $\chi''$ signals (Figure 9), and complex **4** with $Tb^{III}$

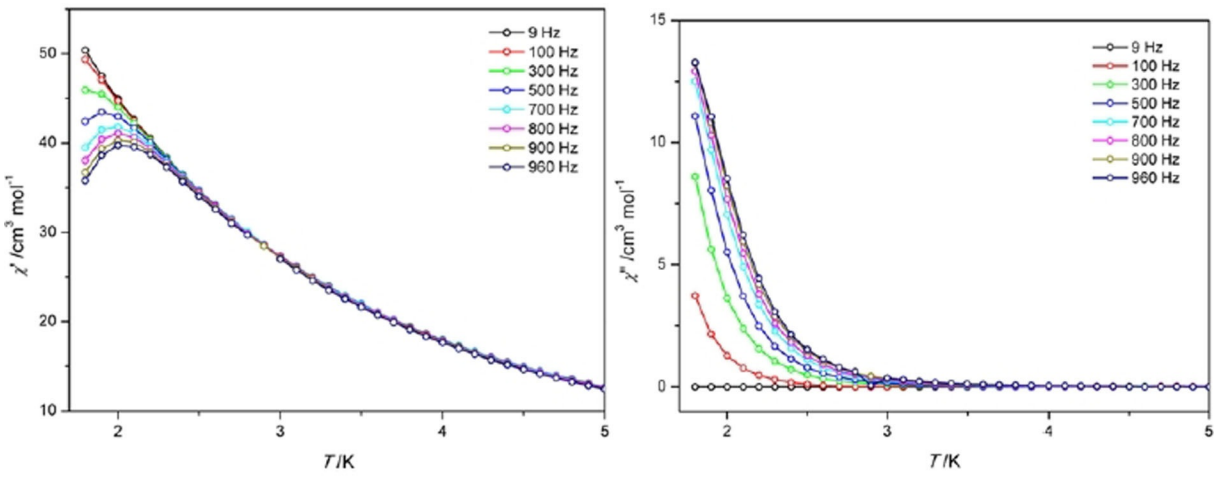


**Figure 7.** The ac susceptibility data for complex **1** at zero dc field.

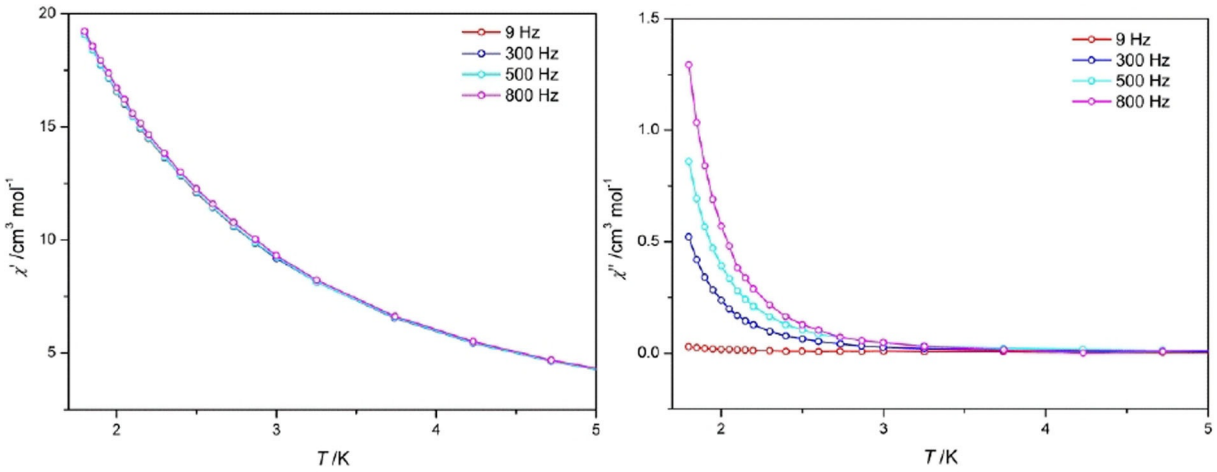


**Figure 8.** The ac susceptibility data for complex **2** at zero dc field.

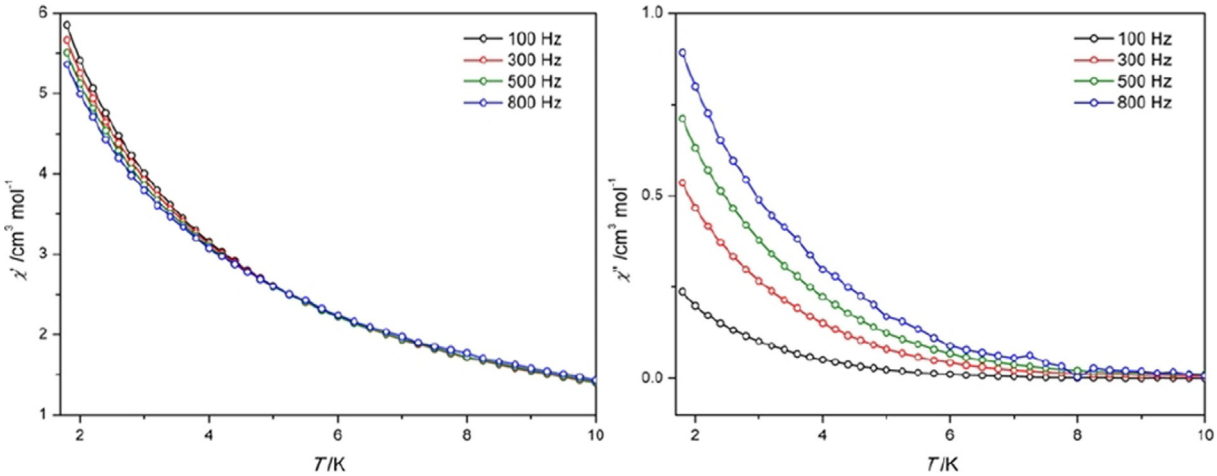


**Figure 9.** The ac susceptibility data for complex **5** at zero dc field.

does not display frequency-dependent $\chi'$ and $\chi''$ signals (Figure S12). These results indicate slow magnetic relaxations in complexes **1**, **2**, and **5**. Complex **1**, incorporating $Cr^{III}$ and $Tb^{III}$ ions, shows slow magnetic relaxation, whereas the similar complex **4** containing $Al^{III}$ and $Tb^{III}$ ions does not. Thus, in this system, the $Cr^{III}$–$Tb^{III}$ ferromagnetic interaction plays an important role in the slow magnetic relaxation for complex **1**. Complex **2** based on $Cr^{III}$ and $Dy^{III}$ ions displays slow magnetic relaxation, and the result can be ascribed to the single-ion behavior of $Dy^{III}$ and/or the $Cr^{III}$–$Dy^{III}$ ferromagnetic interaction. Complex **5** based on $Al^{III}$ and $Dy^{III}$ ions shows a similar behavior without the $Cr^{III}$–$Dy^{III}$ ferromagnetic interaction, probably owing to the single-ion behavior of the $Dy^{III}$ ion.

However, the expected maximum of $\chi''$ lies outside the temperature of 1.8 K, mainly owing to fast QTM. Thus, the energy barrier $U_{eff}$ and relaxation time $\tau_0$ cannot be obtained through the conventional Arrhenius method. Recently, Bartolomé et al. employed another method to obtain the $U_{eff}$ and $\tau_0$, assuming that there is only one relaxation process of the Debye type with one energy barrier and one time constant.[83] Then, with this assumption for complexes **1**, **2**, and **5**, by plotting $\ln(\chi''/\chi')$ versus $1/T$ at the different frequencies, a linear plot according to the equation $\ln(\chi''/\chi') = \ln(2\pi\nu\tau_0) + E_a/k_BT$ serves for the estimation of the energy barrier and the characteristic time (Figures S13 and S14). For complex **1**, these estimates are $U_{eff} \approx E_a/k_B = 17$ K and $\tau_0 = 7 \times 10^{-9}$ s. For complex **2**, the values are $U_{eff} \approx E_a/k_B = 10$ K and $\tau_0 = 1.3 \times 10^{-9}$ s. For complex **5**, we cannot obtain reasonable parameters. Therefore, we performed them in a static magnetic field to probe the effect on relaxation time.[84] As shown in Figure S15, the broad peaks are observed at low frequencies and the relaxation time remain roughly constant, which can be found in many complexes.[71,85] Cole–Cole plots are shown in Figure S16, and show that there is more than one relaxation processes in complex **5**. We chose a moderate magnetic field of 2000 Oe to obtain the ac magnetic susceptibility for complex **5** (Figure S17). Although the expected maxima of $\chi''$ can be observed in out-of-phase magnetic susceptibility, the peaks remain constant as the frequencies increase probably owing to QTM.

## 3. Conclusions

We have described the syntheses, structures, and magnetism of five new hetero-metallic $M^{III}_2Ln^{III}_3$ complexes (**1**–**5**). All complexes possess similar structures, showing a trigonal bipyramidal configuration. Complexes **1** and **2** are associated with 3*d* $Cr^{III}$, incorporating $Tb^{III}$ and $Dy^{III}$, respectively. Complex **3** combines the diamagnetic $Y^{III}$ ion and $Cr^{III}$ in order to elucidate the $Cr^{III}$–$Cr^{III}$ magnetic interaction. Complexes **4** and **5** incorporate the diamagnetic $Al^{III}$ ion in the place of the $Cr^{III}$ ion as diamagnetic "blanks" for complexes **1** and **2**, which were used for the evaluation of the $Cr^{III}$–$Ln^{III}$ magnetic interactions in complexes **1** and **2**. Magnetic measurements reveal that the $Cr^{III}$–$Ln^{III}$ magnetic interactions are strongly ferromagnetic, and the $Cr^{III}$–$Cr^{III}$ magnetic interaction is weak antiferromagnetic. The ac magnetic measurements show that $[Cr^{III}_2Tb^{III}_3]$ (**1**), $[Cr^{III}_2Dy^{III}_3]$ (**2**), and $[Al^{III}_2Dy^{III}_3]$ (**5**) display slow magnetic relaxations, behaving as SMMs. These results enrich the 3*d*–4*f* molecule-based magnetic materials and illustrate the 3*d*–4*f* magnetic nature by incorporating the main-group metal ion by diamagnetic substitution.

## Experimental Section

### Materials and Physical Measurements

All reactions were carried out under aerobic conditions with commercially available chemicals and reagents, which were used as received, without further purification. Elemental analyses for C, H, and N were performed by using an Elementar Vario-EL CHNS elemental analyzer and carried out at Sun Yat-sen University. TG analyses were performed by a NETZSCH TG 209F1 Iris analyzer in Sun Yat-sen University. PXRD data were collected on a D/Max-RA diffractometer (DX-2600, Dan-Dong China) with Cu Kα radiation ($\lambda =$ 1.548 Å) operating at 40 kV and 100 Ma. The magnetic properties were measured on a Quantum Design MPMS-XL7 and a PPMS-9 ACMS magnetometer. Diamagnetic correction was made with Pascal's constants for all constituent atoms.

### Syntheses of Complexes 1–5

#### *{[$Cr_2Tb_3L_{10}(OH)_6(H_2O)_2$]$Et_3NH$} (1)*

$Et_3N$ (0.6 mL) was added to a stirred slurry of HL (0.102 g, 1.0 mmol) and $CrCl_3{\cdot}6H_2O$ (0.2 mmol, 0.053 g) in 15 mL $CH_3CN$. After stirring for 1 h at room temperature, $CH_2Cl_2$ (15 mL) was added and stirred for another 1 h before $Tb(NO_3)_3{\cdot}6H_2O$ (0.3 mmol, 0.135 g) was added. The resulting mixture was heated to reflux for 30 min to give a light purple mixture. The mixture was cooled to room temperature and filtered, and the filtrate was allowed to stand at room temperature. After about 2 weeks, well-shaped purple crystals were obtained, which were subsequently washed with $CH_3CN$ and $CH_2Cl_2$ (10 mL) and dried in air. Yield: 70 mg (34.4%, based on Tb). Elemental analysis: calcd for $Cr_2Tb_3C_{56}H_{116}O_{28}$: C 36.71, H 6.38, N 0.76; found: C 36.89, H 6.80, N 0.48.

#### *{[$Cr_2Dy_3L_{10}(OH)_6(H_2O)_2$]$Et_3NH$} (2)*

The same procedure as complex **1** was used, but with $Dy(NO_3)_3{\cdot}6H_2O$ (0.3 mmol, 0.137 g) in place of $Tb(NO_3)_3{\cdot}6H_2O$. Yield: 42 mg (22.8%, based on Dy). Elemental analysis: calcd for $Cr_2Dy_3C_{56}H_{116}O_{28}$: C36.49, H 6.34, N 0.76; found: C 36.62, H 6.74, N 0.44.

#### *{[$Cr_2Y_3L_{10}(OH)_6(H_2O)_2$]$Et_3NH$} (3)*

The same procedure as complex **1** was used, but with $Y(NO_3)_3{\cdot}6H_2O$ (0.3 mmol, 0.115 g) in place of $Tb(NO_3)_3{\cdot}6H_2O$. Yield: 46 mg (24.5%, based on Y). Elemental analysis: calcd for $Cr_2Y_3C_{56}H_{116}O_{28}$: C 41.46, H 7.21, N 0.86; found: C 41.21, H 7.57, N 0.53.

#### *{[$Al_2Tb_3L_{10}(OH)_6(H_2O)_2$]$Et_3NH{\cdot}H_2O$} (4)*

$Et_3N$ (0.6 mL) was added to a stirred slurry of HL (0.102 g, 1.0 mmol) and $AlCl_3$ (0.2 mmol, 0.027 g) in 15 mL $CH_3CN$. After stirring for 1 h at room temperature, $CH_2Cl_2$ (15 mL) was added and stirred for another 1 h before $Tb(NO_3)_3{\cdot}6H_2O$ (0.3 mmol, 0.135 g)

 

was added. The resulting mixture was heated to reflux for 30 min to give a light purple mixture. The mixture was cooled to room temperature and filtered, and the filtrate was allowed to stand at room temperature. After about 2 weeks, well-shaped purple crystals were obtained, which were subsequently washed with $CH_3CN$ and $CH_2Cl_2$ (10 mL) and dried in air. Yield: 65 mg (33.7%, based on Tb). Elemental analysis: calcd for $Al_2Tb_3C_{56}H_{118}O_{29}$: C 37.36, H 6.61, N 0.78; found: C 37.88 H 6.96, N 0.51.

#### *{[$Al_2Dy_3L_{10}(OH)_6(H_2O)_2$]$Et_3NH{\cdot}H_2O$} (5)*

The same procedure as complex **4** was used, but with $Dy(NO_3)_3{\cdot}6H_2O$ (0.3 mmol, 0.137 g) in place of $Tb(NO_3)_3{\cdot}6H_2O$. Yield: 77 mg (40.8%, based on Dy). Elemental analysis: calcd for $Al_2Dy_3C_{56}H_{118}O_{29}$: C 37.14, H 6.58, N 0.77; found: C 37.51 H 6.88, N 0.46.

### Single-Crystal X-ray Diffraction

The crystal data and cell parameters for **1**–**5** are given in Table 1. Crystallographic data were collected with a SuperNova, Single source at offset (**1**, **2**, **4** and **5**) and Xcalibur (**3**), Eos diffractometers using graphite monochromated Mo/K$\alpha$ radiation ($\lambda = 0.71073$ Å). The data integration and empirical absorption corrections were carried out by SAINT programs. The structure was solved by the SHELXTL 2014 program suite by full-matrix least-square methods on all $F^2$ data.[86] All the non-hydrogen atoms were refined anisotropically on $F^2$ by full-matrix least-squares techniques. All hydrogen atoms, except for those of disordered atoms and lattice water molecules, were generated geometrically and refined isotropically using the riding model. The highly disordered solvent molecules in complexes **1**–**5** were treated by the "SQUEEZE" method as implemented in PLATON,[87] and the results were appended to the CIF files.

The supplementary crystallographic data for this paper were deposited with the Cambridge Crystallographic Data Centre (CCDC) as entry CCDC 1540747 (**1**), 1540748 (**2**), 1540749 (**3**), 1540750 (**4**), and 1540751 (**5**).[88]

## Acknowledgements

*The authors thank the NSFC (21201126), the Subject Construction Project of Sichuan Agricultural University, and the excellent master program of Sichuan Agricultural University (YS2014009).*

## Conflict of Interest

*The authors declare no conflict of interest.*

**Keywords:** 3*d*–4*f* · diamagnetic substitution · ferromagnetic interaction · pentanuclear complexes · slow magnetic relaxation

[1] R. Sessoli, A. K. Powell, *Coord. Chem. Rev.* **2009**, *253*, 2328 – 2341.
[2] D. N. Woodruff, R. E. P. Winpenny, R. A. Layfield, *Chem. Rev.* **2013**, *113*, 5110 – 5148.
[3] M. Evangelisti, E. K. Brechin, *Dalton Trans.* **2010**, *39*, 4672 – 4676.
[4] Y. Z. Zheng, G. J. Zhou, Z. Zheng, R. E. P. Winpenny, *Chem. Soc. Rev.* **2014**, *43*, 1462 – 1475, and references therein.
[5] M. N. Leuenberger, D. Loss, *Nature* **2001**, *410*, 789 – 793.
[6] T. Lis, *Acta Crystallogr. Sect. B* **1980**, *36*, 2042 – 2046.
[7] R. Sessoli, H. L. Tsai, A. R. Schake, S. Wang, J. B. Vincent, K. Folting, D. Gatteschi, G. Christou, D. N. Hendrickson, *J. Am. Chem. Soc.* **1993**, *115*, 1804 – 1816.
[8] R. Sessoli, D. Gatteschi, A. Caneschi, M. A. Novak, *Nature* **1993**, *365*, 141 – 143.
[9] G. Christou, D. Gatteschi, D. N. Hendrickson, R. Sessoli, *MRS Bull.* **2000**, *25*, 66 – 71.
[10] D. N. Hendrickson, G. Christou, H. Ishimoto, J. Yoo, E. K. Brechin, A. Yamaguchi, E. M. S. Rumberger, M. J. Aubin, Z. Sun, G. Aromi, *Polyhedron* **2001**, *20*, 1479 – 1488.
[11] J. P. Price, S. R. Batten, B. Moubaraki, K. S. Murray, *Chem. Commun.* **2002**, 762 – 763.
[12] E. C. Sañudo, W. Wernsdorfer, K. A. Abboud, G. Christou, *Inorg. Chem.* **2004**, *43*, 4137 – 4144.
[13] H. Miyasaka, R. Clérac, W. Wernsdorfer, L. Lecren, C. Bonhomme, K. Sugiura, M. Yamashita, *Angew. Chem. Int. Ed.* **2004**, *43*, 2801 – 2805; *Angew. Chem.* **2004**, *116*, 2861 – 2865.
[14] H. Miyasaka, T. Nezu, K. Sugimoto, K. Sugiura, M. Yamashita, R. Clérac, *Chem. Eur. J.* **2005**, *11*, 1592 – 1602.
[15] C. J. Milios, A. Vinslava, W. Wernsdorfer, S. Moggach, S. Parsons, S. P. Perlepes, G. Christou, E. K. Brechin, *J. Am. Chem. Soc.* **2007**, *129*, 2754 – 2755.
[16] A. M. Mowson, T. N. Nguyen, K. A. Abboud, G. Christou, *Inorg. Chem.* **2013**, *52*, 12320 – 12322.
[17] S. Accorsi, A. L. Barra, A. Caneschi, G. Chastanet, A. Cornia, A. C. Fabretti, D. Gatteschi, C. Mortalo, E. Olivieri, F. Parenti, P. Rosa, R. Sessoli, L. Sorace, W. Wernsdorfer, L. Zobbi, *J. Am. Chem. Soc.* **2006**, *128*, 4742 – 4755.
[18] A. M. Ako, V. Mereacre, Y. Lan, W. Wernsdorfer, R. Clérac, C. E. Anson, A. K. Powell, *Inorg. Chem.* **2010**, *49*, 1 – 3.
[19] Y. Y. Zhu, C. Cui, K. Qian, J. Yin, B. W. Wang, Z. M. Wang, S. Gao, *Dalton Trans.* **2014**, *43*, 11897 – 11907.
[20] C. Mathonière, H. J. Lin, D. Siretanu, R. Clérac, *J. Am. Chem. Soc.* **2013**, *135*, 19083 – 19086.
[21] B. Moubaraki, K. S. Murray, T. A. Hudson, R. Robson, *Eur. J. Inorg. Chem.* **2008**, 4525 – 4529.
[22] K. W. Galloway, A. M. Whyte, W. Wernsdorfer, J. Sanchez-Benitez, K. V. Kamenev, A. Parkin, R. D. Peacock, M. Murrie, *Inorg. Chem.* **2008**, *47*, 7438 – 7442.
[23] A. Ferguson, A. Parkin, J. Sanchez-Benitez, K. Kamenev, W. Wernsdorfer, M. A. Murrie, *Chem. Commun.* **2007**, 3473 – 3475.
[24] M. Murrie, S. J. Teat, H. Stöckli-Evans, H. U. Güdel, *Angew. Chem. Int. Ed.* **2003**, *42*, 4653 – 4656; *Angew. Chem.* **2003**, *115*, 4801 – 4804.
[25] S. K. Langley, M. Helliweel, R. Sessoli, P. Rosa, W. Wernsdorfer, R. E. P. Winpenny, *Chem. Commun.* **2005**, 5029 – 5031.
[26] A. Ferguson, J. Lawrence, A. Parkin, J. Sanchez-Benitez, K. V. Kamenev, E. K. Brechin, W. Wernsdorfer, S. Hill, M. Murrie, *Dalton Trans.* **2008**, 6409 – 6414.
[27] G. Aromí, S. Parsons, W. Wernsdorfer, E. K. Brechin, E. J. L. McInnes, *Chem. Commun.* **2005**, 5038 – 5040.
[28] A. Bell, G. Aromí, S. J. Teat, W. Wernsdorfer, R. E. P. Winpenny, *Chem. Commun.* **2005**, 2808 – 2810.
[29] S. T. Ochsenbein, M. Murrie, E. Rusanov, H. Stoeckli-Evans, C. Sekine, H. U. Güdel, *Inorg. Chem.* **2002**, *41*, 5133 – 5140.
[30] C. Cadiou, M. Murrie, C. Paulsen, V. Villar, W. Wernsdorfer, R. E. P. Winpenny, *Chem. Commun.* **2001**, 2666 – 2667.
[31] A. Ghisolfi, K. Y. Monakhov, R. Pattacini, P. Braunstein, X. López, C. de Graaf, M. Speldrich, J. van Leusen, H. Schilder, P. Kögerler, *Dalton Trans.* **2014**, *43*, 7847 – 7859.
[32] N. Ishikawa, M. Sugita, T. Ishikawa, S. Y. Koshihara, Y. Kaizu, *J. Am. Chem. Soc.* **2003**, *125*, 8694 – 8695.
[33] N. Ishikawa, M. Sugita, W. Wernsdorfer, *Angew. Chem. Int. Ed.* **2005**, *44*, 2931 – 2935; *Angew. Chem.* **2005**, *117*, 2991 – 2995.
[34] P. H. Lin, T. J. Burchell, L. L. Ungur, F. Chibotaru, W. Wernsdorfer, M. Murugesu, *Angew. Chem. Int. Ed.* **2009**, *48*, 9489 – 9492; *Angew. Chem.* **2009**, *121*, 9653 – 9656.
[35] F. Luis, M. J. Martínez-Perez, O. Montero, E. Coronado, S. Cardona-Serra, C. Martí-Gastaldo, J. M. Clemente-Juan, J. Sese, D. Drung, T. Schurig, *Phys. Rev. B* **2010**, *82*, 060403.

 

[36] I. J. Hewitt, J. Tang, N. T. Madhu, C. E. Anson, Y. Lan, J. Luzon, M. Etienne, R. Sessoli, A. K. Powell, *Angew. Chem. Int. Ed.* **2010**, *49*, 6352 – 6356; *Angew. Chem.* **2010**, *122*, 6496 – 6500.
[37] S. K. Langley, N. F. Chilton, B. Moubaraki, K. S. Murray, *Inorg. Chem.* **2013**, *52*, 7183 – 7192.
[38] D. D. Yin, Q. Chen, Y. S. Meng, H. L. Sun, Y. Q. Zhang, S. Gao, *Chem. Sci.* **2015**, *6*, 3095 – 3101.
[39] L. Jia, Y. S. Meng, H. L. Sun, S. Gao, *Chem. Commun.* **2014**, *50*, 6052 – 6055.
[40] Q. Chen, Y. S. Meng, H. L. Sun, Y. Q. Zhang, S. Gao, *Inorg. Chem.* **2016**, *55*, 12904 – 12911.
[41] L. Sun, S. L. Wei, J. Zhang, W. Y. Wang, S. P. Chen, Y. Q. Zhang, Q. Wei, G. Xie, S. L. Gao, *J. Mater. Chem. C* **2017**, *5*, 9488 – 9495.
[42] G. Novitchi, W. Wernsdorfer, L. F. Chibotaru, J. P. Costes, C. E. Anson, A. K. Powell, *Angew. Chem. Int. Ed.* **2009**, *48*, 1614 – 1619; *Angew. Chem.* **2009**, *121*, 1642 – 1647.
[43] J. P. Costes, F. Dahan, W. Wernsdorfer, *Inorg. Chem.* **2006**, *45*, 5 – 7.
[44] F. Mori, T. Nyui, T. Ishida, T. Nogami, K. Y. Choi, H. Nojiri, *J. Am. Chem. Soc.* **2006**, *128*, 1440 – 1441.
[45] S. Osa, T. Kido, N. Matsumoto, N. Re, A. Pochaba, J. Mrozinski, *J. Am. Chem. Soc.* **2004**, *126*, 420 – 421.
[46] C. Aronica, G. Pilet, G. Chastanet, W. Wernsdorfer, J. F. Jacquot, D. Luneau, *Angew. Chem. Int. Ed.* **2006**, *45*, 4659 – 4662; *Angew. Chem.* **2006**, *118*, 4775 – ##4778.
[47] P. Bag, A. Chakraborty, G. Rogez, V. Chadrasekhar, *Inorg. Chem.* **2014**, *53*, 6524 – 6533.
[48] V. Chandrasekhar, B. M. Pandian, R. Boomishankar, A. Steiner, J. J. Vittal, A. Houri, R. Clérac, *Inorg. Chem.* **2008**, *47*, 4918 – 4929.
[49] V. Chandrasekhar, B. M. Pandian, R. Boomishankar, A. Steiner, J. J. Vittal, A. Houri, R. Clérac, *Inorg. Chem.* **2009**, *48*, 1148 – 1157.
[50] S. Dhers, H. L. C. Feltham, M. Rouzières, R. Clérac, S. Brooker, *Dalton Trans.* **2016**, *45*, 18089 – 18093.
[51] M. Ferbinteanu, T. Kajiwara, K. Y. Choi, H. Nojiri, A. Nakamoto, N. Kojima, F. Cimpoesu, Y. Fujimura, S. Takaishi, M. Yamashita, *J. Am. Chem. Soc.* **2006**, *128*, 9008 – 9009.
[52] E. Moreno Pineda, N. F. Chilton, F. Tuna, R. E. P. Winpenny, E. J. L. McInnes, *Inorg. Chem.* **2015**, *54*, 5930 – 5941.
[53] M. Murugesu, A. Mishra, W. Wernsdorfer, K. Abboud, G. Christou, *Polyhedron* **2006**, *25*, 613 – 625.
[54] V. Mereacre, A. M. Ako, R. Clérac, W. Wernsdorfer, G. Filoti, J. J. Bartolomé, C. E. Anson, A. K. Powell, *J. Am. Chem. Soc.* **2007**, *129*, 9248 – 9249.
[55] C. Zaleski, E. Depperman, J. Kampf, M. Kirk, V. Pecoraro, *Angew. Chem. Int. Ed.* **2004**, *43*, 3912 – 3914; *Angew. Chem.* **2004**, *116*, 4002 – 4004.
[56] A. Mishra, W. Wernsdorfer, S. Parsons, G. Christou, E. Brechin, *Chem. Commun.* **2005**, 2086 – 2088.
[57] X. X. He, W. W. Cheng, Q. F. Lin, Y. Y. Dong, Y. Xu, *Cryst. Growth Des.* **2017**, *17*, 347 – 354.
[58] S. Chorazy, B. Sieklucka, S. Ohkoshi, *Cryst. Growth Des.* **2016**, *16*, 4918 – 4925.
[59] C. Cruz, E. Spodine, A. Vega, D. Venegas-Yazigiand, V. Paredes-García, *Cryst. Growth Des.* **2016**, *16*, 2173 – 2182.
[60] J. F. Wu, L. Zhao, L. Zhang, X. L. Li, M. Guo, A. K. Powell, J. K. Tang, *Angew. Chem. Int. Ed.* **2016**, *55*, 15574 – 15578; *Angew. Chem.* **2016**, *128*, 15803 – 15807.
[61] J. F. Wu, L. Zhao, P. Zhang, L. Zhang, M. Guo, J. K. Tang, *Dalton Trans.* **2015**, *44*, 11935 – 11942.
[62] M. L. Kahn, C. Mathoniére, O. Kahn, *Inorg. Chem.* **1999**, *38*, 3692 – 3697.
[63] J. P. Sutter, M. L. Kahn, O. Kahn, *Adv. Mater.* **1999**, *11*, 863 – 865.
[64] M. L. Kahn, P. Lecante, M. Verelst, C. Mathonière, O. Kahn, *Chem. Mater.* **2000**, *12*, 3073 – 3079.
[65] T. Hamamatsu, K. Yabe, M. Towatari, S. Osa, N. Matsumoto, N. Re, A. Pochaba, J. Mroinski, J. L. Gallani, A. Barla, P. Imperia, C. Paulsen, J. P. Kappler, *Inorg. Chem.* **2007**, *46*, 4458 – 4468.
[66] W. T. Chen, G. C. Guo, M. S. Wang, G. Xu, L. Z. Cai, T. Akitsu, M. Akita-Tanaka, A. Matsushita, J. S. Huang, *Inorg. Chem.* **2007**, *46*, 2105 – 2114.
[67] H. L. Gao, B. Zhao, X. Q. Zhao, Y. Song, P. Cheng, D. Z. Liao, S. P. Yan, *Inorg. Chem.* **2008**, *47*, 11057 – 11061.
[68] J. Rinck, G. Novitchi, W. Van den Heuvel, L. Ungur, Y. Lan, W. Wernsdorfer, C. E. Anson, L. F. Chibotaru, A. K. Powell, *Angew. Chem. Int. Ed.* **2010**, *49*, 7583 – 7587; *Angew. Chem.* **2010**, *122*, 7746 – 7750.
[69] T. Birk, K. S. Pedersen, C. Thuesen, T. Weyhermüller, M. Schau-Magnussen, S. Piligkos, H. Weihe, S. Mossin, M. Evangelisti, J. Bendix, *Inorg. Chem.* **2012**, *51*, 5435 – 5443.
[70] C. Thuesen, K. S. Pedersen, M. Schau-Magnussen, M. Evangelisti, J. Vibenholt, S. Piligkos, H. Weihe, J. Bendix, *Dalton Trans.* **2012**, *41*, 11284 – 11292.
[71] S. K. Langley, D. P. Wielechowski, N. F. Chilton, B. Moubaraki, K. S. Murray, *Inorg. Chem.* **2015**, *54*, 10497 – 10503.
[72] S. K. Langley, D. P. Wielechowski, B. Moubaraki, K. S. Murray, *Chem. Commun.* **2016**, *52*, 10976 – 10979.
[73] A. McRobbie, A. R. Sarwar, S. Yeninas, H. M. Nowell, L. Baker, D. Allan, M. Luban, C. A. Muryn, R. G. Pritchard, R. Prozorov, G. A. Timco, F. Tuna, G. F. S. Whitehead, R. E. P. Winpenny, *Chem. Commun.* **2011**, *47*, 6251 – 6257.
[74] S. K. Langley, D. P. Wielechowski, V. Vieru, N. F. Chilton, B. Moubaraki, B. F. Abrahams, L. F. Chibotaru, K. S. A. Murray, *Angew. Chem. Int. Ed.* **2013**, *52*, 12014 – 12019; *Angew. Chem.* **2013**, *125*, 12236 – 12241.
[75] S. K. Langley, C. M. Forsyth, B. Moubaraki, K. S. Murray, *Dalton Trans.* **2015**, *44*, 912 – 915.
[76] S. K. Langley, N. F. Chilton, B. Moubaraki, K. S. Murray, *Chem. Commun.* **2013**, *49*, 6965 – 6967.
[77] A. Upadhyay, S. K. Singh, C. Das, R. Mondol, S. K. Langley, K. S. Murray, G. Rajaraman, M. Shanmugam, *Chem. Commun.* **2014**, *50*, 8838 – 8841.
[78] I. Oyarzabal, J. Ruiz, J. M. Seco, M. Evangelisti, A. Camón, E. Ruiz, D. Aravena, E. Colacio, *Chem. Eur. J.* **2014**, *20*, 14262 – 14269.
[79] S. Alvarez, P. Alemany, D. Casanova, J. Cirera, M. Llunell, D. Avnir, *Coord. Chem. Rev.* **2005**, *249*, 1693 – 1708.
[80] Z. Y. Li, X. Q. Wang, J. J. Zhang, S. Q. Liu, J. Ni, Y. J. Sun, *Eur. J. Inorg. Chem.* **2015**, *34*, 5702 – 5707.
[81] H. Xiang, W. G. Lu, L. Jiang, W. X. Zhang, Y. H. Lan, *Eur. J. Inorg. Chem.* **2016**, *6*, 907 – 912.
[82] S. K. Langley, D. P. Wielechowski, V. Vieru, N. F. Chilton, B. Moubaraki, L. F. Chibotaru, K. S. Murray, *Chem. Sci.* **2014**, *5*, 3246 – 3256.
[83] J. Bartolomé, G. Filoti, V. Kuncser, G. Schinteie, V. Meracre, C. E. Anson, A. K. Powell, D. Prodius, C. Turta, *Phys. Rev. B* **2009**, *80*, 014430.
[84] M. Sugita, N. Ishikawa, T. Ishikawa, S. Koshihara, Y. Kaizu, *Inorg. Chem.* **2006**, *45*, 1299 – 1304.
[85] W. Huang, T. Liu, D. Wu, J. J. Cheng, Z. W. Ouyang, C. Y. Duan, *Dalton Trans.* **2013**, *42*, 15326 – 15331.
[86] G. M. Sheldrick, *Acta Crystallogr.* **2008**, *A64*, 112.
[87] A. L. *J.* Spek, *Appl. Crystallogr.* **2003**, 36, 7 – 13.
[88] CCDC 1540747 (**1**), 1540748 (**2**), 1540749 (**3**), 1540750 (**4**), 1540751 (**5**) contain the supplementary crystallographic data for this paper. These data can be obtained free of charge from The Cambridge Crystallographic Data Centre.

Received: October 20, 2017

 